Proc. Nat. Acad. Sci. USA
Vol. 71, No. 12, pp. 4879–4883, December 1974

Viable Deletion Mutants of Simian Virus 40: Selective Isolation by Means of a Restriction Endonuclease from *Hemophilus parainfluenzae*

(*Hpa* II/plaque-morphology mutants/polyacrylamide gel electrophoresis/heteroduplex mapping)

JANET E. MERTZ AND PAUL BERG

Department of Biochemistry, Stanford University Medical Center, Stanford, California 94305

Contributed by Paul Berg, September 3, 1974

ABSTRACT **Resistance of simian virus 40 (SV40) DNA to cleavage by *Hemophilus parainfluenzae* II (*Hpa*II) restriction endonuclease has been used as a positive, *in vitro* selection for mutants lacking the one *Hpa*II endonuclease-cleavage site of wild-type SV40 DNA. Each of 10 viable mutants isolated by this procedure multiplies significantly more slowly than wild-type virus and contains a small deletion (80 to 190 base pairs in size) of the region of the genome that includes the *Hpa*II endonuclease-recognition sequence. These well-defined mutants, having a selective disadvantage for growth, would not have been readily obtained by conventional methods used to screen for viral mutants. Therefore, in certain circumstances, restriction endonucleases are effective reagents for the selection of new classes of mutants. Because these small deletions can be visualized in heteroduplexes, these mutants provide internal markers for mapping other alterations or features of the simian virus 40 genome.**

Type II restriction endonucleases are enzymes that make double-strand scissions at specific nucleotide sequences in duplex DNA (see ref. 1 for review). This property has been used for the *in vitro* selection of viral mutants that are resistant to cleavage by a restriction endonuclease because they have deleted the nucleotide sequence recognized by the enzyme (2). In this paper we describe the isolation and physical characterization of a set of naturally arising mutants of simian virus 40 (SV40) that lack the nucleotide sequence recognized by *Hpa*II restriction endonuclease, an enzyme from *Hemophilus parainfluenzae* that cleaves wild-type SV40 DNA once at a unique site on the genome (3). Each of the mutants described here is *viable* (although it multiplies more slowly than wild-type SV40) and contains a small (80 to 190 base pairs) deletion of the region that includes the *Hpa*II endonuclease-cleavage site. The isolation of clones of *non-viable*, *Hpa*II endonuclease-resistant mutants containing large deletions that include this region of the SV40 genome has been reported elsewhere (2).

MATERIALS AND METHODS

Cells, Viruses, and DNAs. Monkey kidney cell lines were obtained and grown as already described (2). Stocks of wild-type (*WT800*) and mutant virus and DNA were prepared, purified and titered as previously described (2).

Enzymes and Enzyme Reactions. (*a*) *Eco*RI restriction endonuclease (4, 5), a gift from M. Thomas and J. Ferguson, was used under conditions previously described (6). (*b*) *H. parainfluenzae* I (*Hpa*I) restriction endonuclease, purified by the procedure of Sharp *et al.* (3), was a gift from J. Carbon. SV40 Form I DNA was treated with the enzyme for 1 hr at 37° in 20 μl reaction mixtures containing 10 mM Tris·HCl (pH 7.5), 10 mM $MgCl_2$, 6 mM KCl, 1 mM dithiothreitol, and 100 μg/ml of gelatin (autoclaved, Difco-Bacto). (*c*) *Hpa*II restriction endonuclease, prepared from *H. parainfluenzae* cells by a modification of the second method of Sharp *et al.* (3), was the enzyme preparation previously described (2). Reactions with *Hpa*II endonuclease were performed for 1–4 hr at 37° in 10 mM Tris·HCl (pH 7.5), 5 mM $MgCl_2$, 0.4 mM dithiothreitol, and 100 μg/ml of gelatin. To insure complete digestion, the endonuclease-resistant DNA was purified by equilibrium centrifugation in CsCl–ethidium bromide (7) and re-incubated with additional *Hpa*II endonuclease. (*d*) The restriction enzyme preparation obtained from *Hemophilus influenzae* strain d (8), containing a mixture of the *Hin*dII and *Hin*dIII endonucleases (9), was a gift from H. F. Tabak (10). Reactions were performed for 30 min at 37° in 30 μl containing SV40 Form I DNA (approximately 1 μg), 5 mM Tris·HCl (pH 7.4), 7 mM $MgCl_2$, 50 mM NaCl, 1 mM dithiothreitol, and 2 μl of enzyme, and stopped by adding EDTA and sodium dodecyl sulfate to final concentrations of 25 mM and 1%, respectively.

Electron Microscopy was performed by the formamide technique of Davis *et al.* (11).

Polyacrylamide Gel Electrophoresis was performed essentially as described by Tabak *et al.* (10) with 4% cylindrical gels (0.65 × 15 cm).

RESULTS

Resistance to cleavage by *Hpa*II restriction endonuclease selects for variant SV40 DNA molecules that exhibit altered plaque phenotypes

Serial passaging of SV40 in monkey cells at high multiplicities of infection results in the accumulation of defective virions that contain deletions, substitutions, and additions in their DNA (12, 13). Since these alterations vary greatly in size and are located nearly randomly throughout the viral genome (14, 15), such defective SV40 DNA preparations provide a potential source of mutants. When our wild-type SV40 virus was serially passaged four times in primary African green monkey kidney cells at high input multiplicities of infection, 47% of the SV40 DNA molecules in the resulting preparation were found to be resistant to cleavage by *Hpa*II restriction endonuclease, an enzyme that cleaves wild-type SV40 DNA molecules once at map position 0.735 (see Fig. 3). After sepa-

Abbreviation: SV40, simian virus 40.

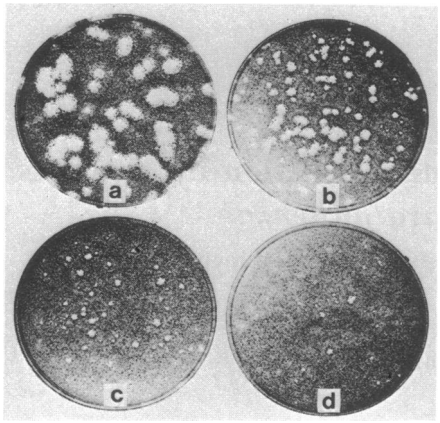

FIG. 1. Size of plaques seen 12 days after infection with wild type (a) and *Hpa*II endonuclease-resistant mutants (b–d). Monolayers of CV-1P cells were infected with approximately 50 plaque-forming units of the indicated virus, overlayed with agar medium, and then incubated at 37° as previously described (2); neutral red was added 9 days after infection. (a) *WT800;* (b) *pm(dl)801;* (c) *pm(dl)802;* (d) *pm(dl)805.*

ration from the cleaved linear DNA by equilibrium centrifugation in CsCl–ethidium bromide, this *Hpa*II endonuclease-resistant DNA preparation produced 10^4-fold fewer plaques per μg than wild-type SV40 DNA when assayed by the DEAE-dextran method of McCutchan and Pagano (16) because of the defectiveness of the viral genomes (see Table 1 of ref. 2). The residual plaques seen could have been produced by a contaminating trace of wild-type DNA; however, many of them appeared later and grew more slowly in size than ones derived from wild-type molecules.

Sixteen of these plaques were picked. After three serial plaque-purifications of each isolate, virus and viral DNA stocks were prepared from cells infected at low multiplicities

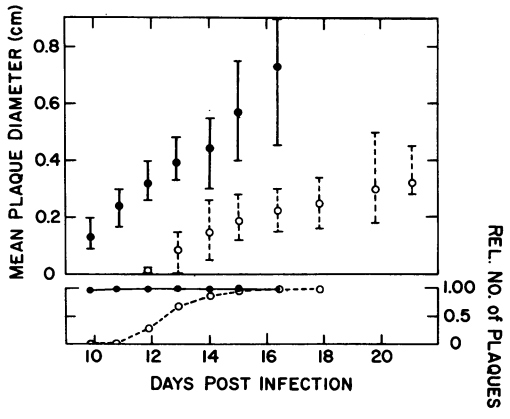

FIG. 2. Rate of growth and time of appearance of *WT800* (●) and *pm(dl)806* (○) plaques. Plaque assays were performed with CV-1P cells as described in the legend to Fig. 1. Plaque diameters were approximate measurements made with a ruler of the diameter of the "white" regions of plaques seen after staining the cells with neutral red; plaques were assumed to be roughly circular in shape. Mean plaque diameters are average sizes of 6 to 12 plaques selected for measurement at random; horizontal bars indicate the range of sizes recorded on a given day. The number of plaques recorded each day was determined relative to the number of plaques observed sixteen days post-infection [27 and 51 per dish for *WT800* (●) and *pm(dl)806* (○), respectively].

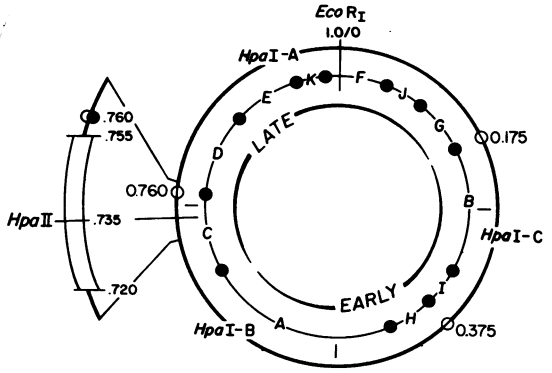

FIG. 3. Map of SV40 showing the cleavage sites of several restriction endonucleases and the location of the DNA segment deleted from mutant *pm(dl)810.* The inner circle shows the locations of the *Hin*dII+III endonuclease-cleavage sites (●) and the corresponding DNA fragments (A through K) that result from cleavage with this pair of enzymes (9). The outer circle shows the map positions of the *Hpa*I endonuclease-cleavage sites (○) and the DNA fragments produced after cleavage at these sites (3, 9). Map coordinates are expressed as SV40 DNA fractional length; the 0 position is defined by the one unique *Eco*RI endonuclease-cleavage site (9, 24). *Hpa*II endonuclease cleaves at map position 0.735 (3, 25). The early and late regions of the genome are from the data of Dhar *et al.* (26).

of infection. Ten of the virus isolates reproducibly yielded late-appearing, small plaques when assayed on the monkey cell line CV-1P; the remaining six stocks produced plaques that were indistinguishable from those of wild-type virus. Examination of the rate at which the plaques of each of these 10 SV40 variants developed, as judged either, subjectively, by the size of the plaques seen 12 days after infection (Fig. 1) or, quantitatively, by direct measurement of the rate at which the average diameter of the plaques increased (Fig. 2, Table 1), showed that their plaque growth rates span a substantial range. Even in a single cycle of growth, replication of the mutant DNAs occurs more slowly than that of wild-type DNA (J. E. Mertz, S. P. Goff, and P. Berg, unpublished).

As anticipated, the DNA isolated from each of the 10 plaque-morphology mutants [hereafter referred to as *pm(dl)*-

TABLE 1. *Rate of growth of the plaques of HpaII endonuclease-resistant mutants: Mean plaque diameters in mm**

Mutant	Days post infection					
	9.9	10.8	11.8	12.8	15.1	17.8
WT800	1.4	2.4	3.2	3.9	5.6	ND
pm(dl)801	0.9	1.8	2.6	3.7	4.4	ND
pm(dl)802	0.5	0.9	1.3	1.9	2.9	4.3
pm(dl)803	0.3	0.9	1.8	2.6	3.8	5.6
pm(dl)804	0.2	0.9	1.3	1.9	3.3	4.4
pm(dl)805	0.3	1.0	1.3	1.9	3.1	4.3
pm(dl)806	<0.1	<0.1	0.3	0.9	1.9	2.5
pm(dl)807	0.3	1.2	2.4	2.9	3.5	5.4
pm(dl)808	0.5	1.4	2.4	3.2	4.2	5.6
pm(dl)809	0.5	1.2	2.0	2.6	3.7	ND
pm(dl)810	<0.1	0.4	1.2	2.2	3.4	4.1

ND, not determined.
* Determined as described in the legend to Fig. 2.

801 through *pm(dl)810*, where "*pm*" = plaque-morphology and "*dl*" = deletion (17)] was completely *resistant* (>99%) to cleavage by *Hpa*II endonuclease, whereas the DNA from each of the six isolates that produced wild-type plaques was almost completely cleaved (>98%) by the enzyme to unit length linear SV40 DNA. Thus, resistance to cleavage by *Hpa*II endonuclease serves as an efficient, positive, *in vitro* selection for the isolation of *viable*, SV40 plaque-morphology mutants whose DNAs lack that restriction enzyme-cleavage site. [*Non-viable*, defective mutants with extensive deletions of the region of the genome that includes the *Hpa*II endonuclease-cleavage site have also been isolated by this procedure, but these mutants can only grow when complemented by a suitable helper virus (2).]

The *Hpa*II endonuclease-resistant plaque morphology mutants have deleted a small region of the SV40 genome that includes the *Hpa*II endonuclease-cleavage site

Is the DNA of each of these plaque-morphology mutants resistant to cleavage by *Hpa*II endonuclease because of base pair changes in the nucleotide sequence recognized by the enzyme or because of more extensive alterations (e.g., deletions) that modify or eliminate the restriction site? An examination of the contour lengths of *pm(dl)810* and *WT800* DNA by electron microscopy (with bacteriophage PM2 DNA serving as an internal length standard) revealed that *pm(dl)-810* DNA is 96.7 ± 0.2% [mean ± standard error (SEM); standard deviation (σ) = 3%] the length of wild-type DNA, suggesting that a small region of the viral genome had been deleted from this mutant.

To obtain a more accurate estimate of the size and location of the molecular change in each mutant's genome, we compared the electrophoretic mobilities of the DNA fragments produced by cleavage of the mutant and wild-type DNAs with *Hin*dII+III restriction endonuclease. These two enzymes together cleave wild-type SV40 DNA into eleven fragments labeled *Hin*d-A through K in order of their size (see Fig. 3). Since the *Hpa*II endonuclease-cleavage site is contained within *Hin*d fragment C (Fig. 3), a mutant with a deletion of this region should yield a faster migrating *Hin*d-C fragment. On the other hand, base changes should alter the *Hin*dII+III fragment pattern only if they create new, or eliminate old, *Hin*dII+III endonuclease-cleavage sites. Co-electrophoresis of the *Hin*dII+III endonuclease digest products of wild-type and each of the 10 mutant DNAs revealed no significant differences in the mobility or relative quantity of 10 of the 11 *Hin*dII+III endonuclease-generated fragments. However, instead of the normal *Hin*d-C fragment, each of the mutant DNAs showed one new, faster migrating fragment (designated *Hin*d-C') (Fig. 4; Table 2).* Therefore, each mutant has an alteration in the *Hin*dII+III DNA fragment that contains the *Hpa*II endonuclease-cleavage site. Furthermore, the faster migration rate of these new fragments, combined with the fact that the relative electrophoretic mobility of DNA is generally related inversely to molecular length,† suggests that the alteration in each mutant is a deletion within the *Hin*d-C fragment that results in a shorter *Hin*d fragment C.

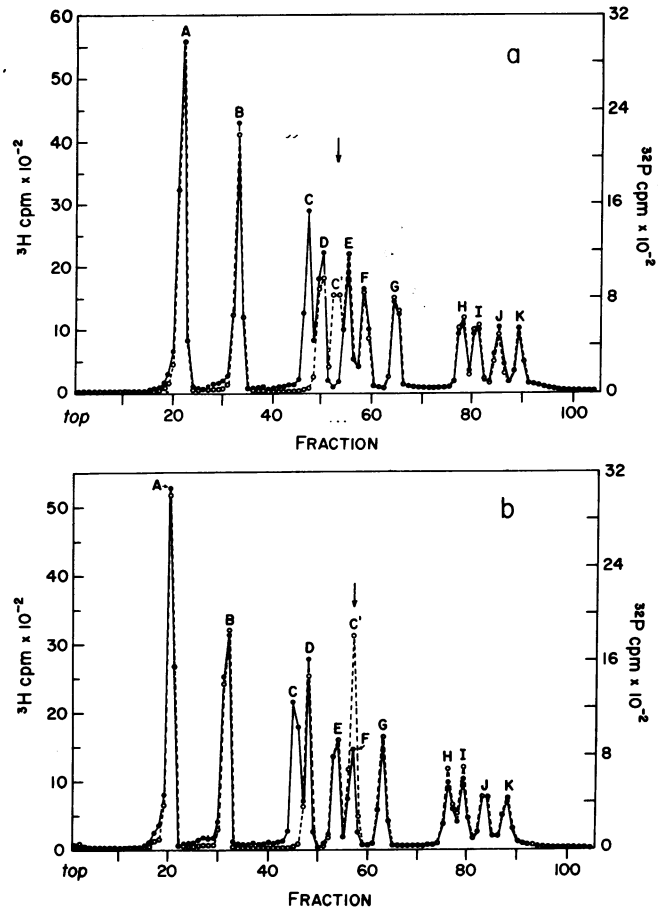

FIG. 4. Polyacrylamide gel electrophoresis patterns of the DNA fragments produced by cleavage of (^{32}P) *WT800* (●——●) and (^{3}H) mutant (O- - -O) DNA with *Hin*dII+III restriction endonuclease. *WT800* [^{32}P]DNA (labeled *in vivo* with inorganic [^{32}P]phosphate) and *pm(dl)801* (a) or *pm(dl)805* (b) [^{3}H]DNA were mixed, treated with *Hin*dII+III restriction endonuclease, and electrophoresed at room temperature for 13.3 hr in 4% polyacrylamide gels at 3.5 mA per gel as described in *Methods*. The letters above each peak correspond to those in Fig. 3 that indicate their locations on the SV40 map (9). ●, ^{32}P; O, ^{3}H.

The sizes of the DNA fragments produced by cleavage of the mutant DNAs with *Hpa*I restriction endonuclease, an enzyme that cleaves wild-type SV40 DNA at three sites (see Fig. 3), were also examined. As expected, the *Hpa*I-A and C fragments were unaltered in their electrophoretic mobility in 1.3% agarose gels, but the third fragment resulting from each mutant migrated more rapidly than *Hpa*I-B, the fragment that contains the *Hin*d-C segment (Fig. 3) (data not shown).

* We have assumed that the *WT800 Hin*d fragments A through K designated in Fig. 4 correspond to the analogous *Hin*d A through K fragments mapped by Danna *et al.* (9) for SV40 strain 776; in actuality, the *WT800 Hin*d fragments A, B and C migrate significantly more slowly and *Hin*d-F more rapidly than their counterparts in strain 776 (Mertz and Berg, unpublished).

† This correlation may not be strictly valid, since differences in G+C content affect the mobility of DNA in polyacrylamide gels (22). Note that the mobility of the *Hin*d-C and F fragments, containing the highest and one of the lowest G+C contents, respectively (23), deviates significantly from the curve relating mobility to molecular length (Fig. 5); in fact, *Hin*d-F migrates more slowly than *Hin*d-G even though *Hin*d-F is the *smaller* of the two fragments.

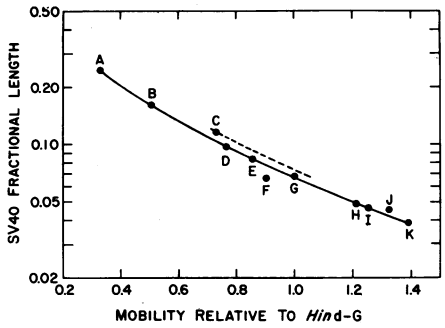

FIG. 5. Correlation between molecular weight and electrophoretic mobility in 4% polyacrylamide gels of the *Hind*II+III fragments of *WT800* SV40 [^{32}P]DNA. The data were determined by averaging the values obtained from 9 gels similar to those in Fig. 4. The relative mobility of each fragment was calculated as its distance from the origin divided by the distance of fragment G from the origin. Molecular weights were determined from the percent of the total radioactivity (excluding estimated background) in each fragment; the value (% of SV40 DNA) obtained for each of the *Hind* fragments was: A, 23.74 ± 0.09 (mean ± SEM); B, 15.79 ± 0.06; C, 11.28 ± 0.08; D, 9.65 ± 0.09; E, 8.32 ± 0.07; F, 6.56 ± 0.04; G, 6.80 ± 0.06; H, 4.82 ± 0.09; I, 4.62 ± 0.06; J, 4.51 ± 0.06; and K, 3.89 ± 0.04.

By assuming that the mobility of the *Hind*-C′ fragment of each mutant reflects its size and that the difference in the relative mobilities of *Hind*-C and *Hind*-C′ measures the difference in their size, one can calculate the approximate size of the deletion in the genome of each mutant (Fig. 5; Table 2): each of the plaque-morphology mutants lacks a small region (80 to 190 base pairs) of DNA contained in the wild-type *Hind*-C and *Hpa*I-B fragments.

The precise map position of these small deletions can be determined by heteroduplex analysis

For mapping accurately the location of these deletions, approximately equal quantities of *Eco*RI restriction endonuclease-generated linear DNA molecules of mutant *pm(dl)810* and *WT800* were mixed together, denatured, renatured, and examined by electron microscopy. Forty percent of the duplexes seen contained one small discontinuity in their structure (Fig. 6A). These discontinuities probably represent deletion loops in the heteroduplexes because most of them (42 out of the 48 that were measured) occur at a unique position 0.245 ± 0.001 (mean ± SEM; σ = 0.007) SV40 fractional length from the nearer *Eco*RI endonuclease-generated end (Fig. 6B). These data, together with the estimate of the size of the DNA segment deleted from the *Hind*-C fragment (see above; Table 2), indicate that the deletion in mutant *pm(dl)810* begins at approximately 0.720, extends to 0.755 on the SV40 map, and includes the *Hpa*II endonuclease-cleavage site at 0.735 (Fig. 3). Therefore, this mutant is resistant to cleavage by *Hpa*II endonuclease because it lacks the region of wild-type SV40 DNA containing that restriction endonuclease-recognition sequence.

In a similar manner, the DNA segment missing in mutant *pm(dl)808* has been located at 0.723 to 0.758 (SEM = 0.001, σ = 0.007) on the SV40 map. Our inability to detect any specific discontinuities in heteroduplexes formed between the DNAs of these two mutants by conventional electron microscopic techniques is consistent with the extensive overlap in the map positions of the deletions present in *pm(dl)808* and *pm(dl)810*. Furthermore, that the *only* region of non-homology in heteroduplexes formed between *pm(dl)808* and *WT800* DNA occurs at this map position has been shown using S1 enzyme (18), a single-strand-specific nuclease that can make double-strand scissions at mismatches present in duplexed DNA molecules (19). Therefore, the peculiar phenotype of this mutant must result from this one mapped alteration in the structure of its DNA.

TABLE 2. *Size of the DNA segments deleted from HpaII endonuclease-resistant plaque-morphology mutants of SV40*

Mutant	Mobility of *Hind*-C′ relative to *Hind*-G*	Estimated size of *Hind*-C′ (% of SV40 DNA)†	Estimated deletion size‡ (nucleotide pairs)
WT800	0.725 ± 0.002§	11.28 ± 0.08§	—
pm(dl)801	0.815	9.75	80
pm(dl)802	0.817	9.75	80
pm(dl)803	0.823	9.65	85
pm(dl)804	0.888	8.65	135
pm(dl)805	0.903	8.40	150
pm(dl)806	0.910	8.30	150
pm(dl)807	0.919	8.15	160
pm(dl)808	0.956	7.70	185
pm(dl)809	0.960	7.65	185
pm(dl)810	0.964	7.60	190

* (Distance of mutant's *Hind*-C′ DNA fragment from origin) ÷ (distance of *Hind*-G fragment from origin); mobilities were determined from electropherograms similar to those in Fig. 4.

† Estimated using the broken line in Fig. 5 that was drawn through the *Hind*-C fragment parallel to the solid line. By using this line, we have assumed that the mobilities of the various *Hind*-C′ fragments deviate from the standard curve to the same extent as does the *Hind*-C fragment; if the deletion substantially changes the G+C content of the C fragment, this assumption is not valid.

‡ Calculated from the difference in size between *Hind*-C and each *Hind*-C′ fragment, assuming that wild-type SV40 DNA contains 5100 base pairs.

§ Data from Fig. 5.

DISCUSSION

This paper describes the isolation of 10 plaque-morphology, deletion mutants of SV40 by a positive selection procedure: the *in vitro* resistance of mutant DNA to cleavage by *Hpa*II restriction endonuclease. Viable plaque-morphology mutants of SV40 have previously been described (see refs. 20 and 21, for examples), but these are the first such mutants isolated using a positive selection and for which the alteration in the genome has been well defined. Recently, SV40 mutants containing an *insertion* of poly(dA)·poly(dT) at the *Hpa*II endonuclease-cleavage site have been "constructed" *in vitro* (15); these mutants behave physiologically similar to the ones described in this paper. Hopefully, procedures similar to these will greatly facilitate the isolation of mutants that could not otherwise be readily obtained.

The nature of these mutants' physiological defect(s) is, as yet, unknown. The fact that there is not a positive correlation between the size of the deleted region and the defectiveness of the mutant as measured by plaque growth rate [e.g., compare mutants *pm(dl)806* and *pm(dl)808* (Tables 1 and 2)] indicates that the exact location, rather than absolute size,

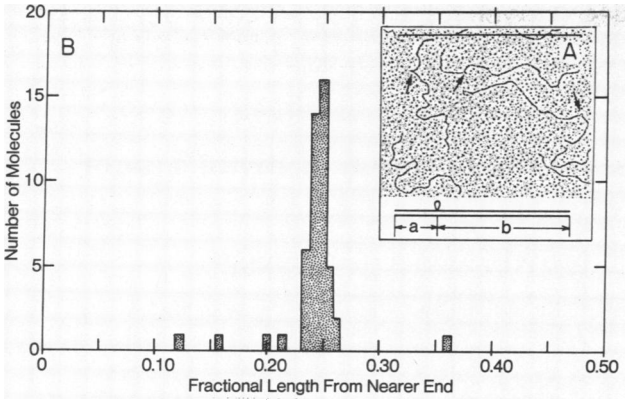

FIG. 6. (A) Electron micrograph of heteroduplexes formed between *Eco*RI endonuclease-cleaved *WT800* and mutant *pm(dl)810* DNA. Approximately equal amounts of *Eco*RI endonuclease-cut linear SV40 DNA from *WT800* and *pm(dl)810* were mixed together, denatured in alkali, annealed at room temperature in 47% formamide, and spread for electron microscopy from 40% formamide (11). Grids were examined as previously described (6). The schematic diagram depicts the presumed structure of the heteroduplexes. The *arrows* point to the putative deletion loops. The *black bar* at the top indicates the size of unit length duplexed SV40 DNA. (B) Histogram of the measured distances from the nearer *Eco*RI endonuclease-generated ends to the putative deletion loops. Double-stranded DNA molecules resulting from the experiment described in (A) were photographed at random. Lengths "a" and "b" were measured for all duplexed molecules that contained discontinuities similar to those indicated by *arrows* in panel A. The fractional length of the beginning of each putative deletion loop to the nearer of the two ends was calculated as equal to a/((a+b)/0.965), assuming that the length of *pm(dl)810* DNA, a+b, equals 0.965 SV40 fractional length.

of the deletion may be the crucial factor determining a given mutant's specific phenotype.

These mutants are particularly useful because they provide an easily recognizable marker for heteroduplex analysis of SV40 DNA. Since the only structural anomaly reproducibly seen by electron microscopy in heteroduplexes between *pm(dl)808* and *WT800* or SV40 strain SV-S (20) DNA occurs at the *Hpa*II endonuclease-cleavage site (Mertz and Berg, unpublished), this feature and the *Eco*RI endonuclease-generated ends together can serve as markers for unambiguously mapping other alterations in the SV40 genome (e.g., the location of deletions in uncloned populations of defective SV40 genomes). Because these deletion loops are so small, one must be cautious and take care to distinguish them from similar-appearing artifacts of electron microscopy (e.g., cytochrome *c* aggregates).

We wish to thank M. Dieckmann, J. Carbon and T. Shenk for help with some of the experiments. This work was supported in part by research grants from the U.S. Public Health Service (GM 13235 and 5 TI GM 196) and the American Cancer Society (VC 23C). J.E.M. is a U.S. Public Health Service Trainee.

1. Meselson, M., Yuan, R. & Heywood, J. (1972) *Annu. Rev. Biochem.* **41**, 447–466.
2. Mertz, J. E. & Berg, P. (1974) *Virology*, in press.
3. Sharp, P. A., Sugden, B. & Sambrook, J. (1973) *Biochemistry* **12**, 3055–3063.
4. Greene, P. J., Betlach, M. C., Goodman, H. M. & Boyer, H. W. (1974) in *Methods in Molecular Biology*, ed. Wickner, R. B. (Marcel Dekker, Inc., New York), Vol. 9, in press.
5. Smith, H. O. & Nathans, D. (1973) *J. Mol. Biol.* **81**, 419–423.
6. Mertz, J. E. & Davis, R. W. (1972) *Proc. Nat. Acad. Sci. USA* **69**, 3370–3374.
7. Radloff, R., Bauer, W. & Vinograd, J. (1967) *Proc. Nat. Acad. Sci. USA* **57**, 1514–1521.
8. Smith, H. O. & Wilcox, K. (1970) *J. Mol. Biol.* **51**, 379–391.
9. Danna, K. J., Sack, G. H., Jr. & Nathans, D. (1973) *J. Mol. Biol.* **78**, 363–376.
10. Tabak, H. F., Griffith, J., Geider, K., Schaller, H. & Kornberg, A. (1974) *J. Biol. Chem.* **249**, 3049–3054.
11. Davis, R., Simon, M. & Davidson, N. (1971) in *Methods in Enzymology*, eds. Grossman, L. & Moldave, K. (Academic Press, New York), Vol. 21, pp. 413–428.
12. Yoshiike, K. (1968) *Virology* **34**, 391–401.
13. Tai, H. T., Smith, C. A., Sharp, P. A. & Vinograd, J. (1972) *J. Virol.* **9**, 317–325.
14. Risser, R. & Mulder, C. (1974) *Virology* **58**, 424–438.
15. Mertz, J. E., Carbon, J., Herzberg, M., Davis, R. W. & Berg, P. (1974) *Cold Spring Harbor Symp. Quant. Biol.* **39**, in press.
16. McCutchan, J. H. & Pagano, J. S. (1968) *J. Nat. Cancer Inst.* **41**, 351–357.
17. Robb, J. A., Tegtmeyer, P., Martin, R. G. & Kit, S. (1972) *J. Virol.* **9**, 562–563.
18. Ando, T. (1966) *Biochim. Biophys. Acta* **114**, 158–168.
19. Shenk, T. E., Rhodes, C., Rigby, P. W. J. & Berg, P. (1974) *Cold Spring Harbor Symp. Quant. Biol.* **39**, in press.
20. Takemoto, K. K., Kirschstein, R. L. & Habel, K. (1966) *J. Bacteriol.* **92**, 990–994.
21. Dubbs, D. R. & Kit, S. (1968) *J. Virol.* **2**, 1272–1282.
22. Zeiger, R. S., Salomon, R., Dingman, C. W. & Peacock, A. C. (1972) *Nature New Biol.* **238**, 65–69.
23. Danna, K. J. & Nathans, D. (1972) *Proc. Nat. Acad. Sci. USA* **69**, 3097–3100.
24. Morrow, J. F., Berg, P., Kelly, T. J., Jr. & Lewis, A. M., Jr. (1973) *J. Virol.* **12**, 653–658.
25. Morrow, J. F. & Berg, P. (1973) *J. Virol.* **12**, 1631–1632.
26. Dhar, R., Subramanian, K., Zain, S., Pam, J. & Weissman, S. M. (1974) *Cold Spring Harbor Symp. Quant. Biol.* **39**, in press.